A. Zanotti, G. Droandi, F. Auteri, G. Gibertini, A. Le Pape
Robustness and Limits of Vortex Generator Effectiveness in Helicopter Drag Reduction
Journal of the American Helicopter Society, Vol. 61, N. 3, 2016, 032007 (7 pages)

Robustness and Limits of Vortex Generators Effectiveness in Helicopter Drag Reduction

Alex Zanotti

Post-Doc Fellow

Giovanni Droandi

Post-Doc Fellow

Franco Auteri

Associate Professor

Giuseppe Gibertini

Assistant Professor

Politecnico di Milano

Dipartimento di Scienze e Tecnologie Aerospaziali

via La Masa 34, Milan, Italy

Arnaud Le Pape

Research Scientist

ONERA - The French Aerospace Lab

Applied Aerodynamics Department

8 Rue des Vertugadins, F-92190, Meudon, France

Abstract

The effect of vortex generators on helicopter drag was investigated in a wind tunnel test. An array of counter-rotating vortex generators was mounted on the rear ramp of a heavy-class helicopter model, slightly downstream of the fuselage upsweep. The wind tunnel campaign also included tests with a radome positioned upstream of the vortex generators to evaluate the robustness of the vortex generators. At cruise angle of attack, a drag reduction of about 2% with respect to the complete helicopter configuration was measured for the baseline fuselage configuration with the vortex generator array installed. The range of angles of attack and sideslip where the vortex generators were effective for drag reduction was established. The addition of a radome mounted upstream on the fuselage lower side renders the vortex generators ineffective. However, for the model attitudes where the vortex generators were ineffective, the vortex generators did not increase helicopter drag. Steady and unsteady pressures measured on the fuselage rear ramp revealed the flow behavior due to the presence of the vortex generators.

Nomenclature

C_D drag coefficient

C_{Dc} drag coefficient measured for the complete upright model with rotating hub at cruise angle of attack

C_p pressure coefficient

f frequency [Hz]

F.S. full-scale

L fuselage width [m]

M Mach number

p [Pa] pressure

St Strouhal number, fL/V_∞

V_∞ free-stream velocity [m/s]

X [m] stream-wise coordinate

Y [m] span-wise coordinate

Z [m] vertical coordinate

α [deg] angle of attack

β [deg] sideslip angle

δ [m] boundary layer displacement thickness

Introduction

In order to reduce the environmental impact caused by the increased use of aircraft, recent research activity was spurred towards finding new solutions for drag reduction to reduce the fuel consumption and, consequently, polluting emissions. The investigation of active flow control devices for the suppression of the recirculating flow region over the fuselage back-ramp was the topic of different comprehensive activities combining computational and experimental effort to study drag reduction on a generic rotorcraft fuselage. In particular, in the recent years, experimental activities were performed to investigate the effectiveness of air-jet blowing devices positioned over the back-ramp region [1, 2]. Indeed, wind tunnel tests demonstrated that a significant drag and download reduction could be obtained over a wide range of angles of attack through the use of different flow control strategies. Numerical simulations were also performed in a collaborative investigation between ONERA and NASA to evaluative the effectiveness of different Navier-Stokes codes to predict the trends observed in these experiments [3]. The comparison of numerical results with experimental data demonstrated that the employed flow solvers were able to predict the overall flow features without capturing quantitatively the fuselage forces or performance of the flow control.

Aircraft drag reduction becomes one of the main topics of investigation of the CleanSky Programme, funded by the European Union. In the Green RotorCraft (GRC) Programme, representing the branch of the CleanSky Programme related to rotorcraft, several solutions were developed and studied to reduce helicopter drag. Among several possibilities, the use of simple passive devices such as vortex generators (VGs) [4] represents a very interesting solution for drag reduction of blunt helicopter fuselages, due to the easy and low-cost installation. Minimal effort has been spent to date on the study of VGs for helicopter drag reduction. In the framework of GRC2 CleanSky Programme, experimental and numerical activities were planned to investigate the use of vortex generators for helicopter fuselage drag reduction. In particular, the first task was the design of suitable solutions by means of CFD simulations. ONERA proposed a solution based on a single array of counter-rotating vortex generators attached on the back ramp of a heavy-class helicopter [5]. The pronounced upsweep of the after-body shape that characterizes blunt fuselages is responsible for a recirculating region at the junction with the tail boom, yielding penalties on helicopter drag. This study was focused on a helicopter attitude close to cruise condition, i.e. with zero angle of attack and sideslip. CFD results showed a non-negligible reduction of about 2% of the complete helicopter drag computed with this VG configuration at cruise attitude. After the CFD assessment, an experimental campaign was performed in the large wind tunnel of Politecnico di Milano to validate the numerical predictions. CFD results computed at cruise attitude with counter-rotating vortex generators installed were confirmed by the wind tunnel tests [6]. Based on these promising results, the robustness of the VG effectiveness (sensitivity to variations in the angle of attack and sideslip, as well as to flow disturbances produced by an upwind external device) was further tested.

In this paper, wind tunnel tests results are presented showing the range of angles of attack and sideslip where the VGs are effective for drag reduction. Fuselage loads measurements are complemented by steady and unsteady pressures measured on the fuselage back-ramp providing a detailed insight into the flow behavior caused by the presence of the VGs.

Experimental set up

The experimental activity was carried out in the large wind tunnel of Politecnico di Milano (LGV). The LGV test section dimensions are 4 m $\times$ 3.84 m. The maximum wind velocity is 55 m/s and the turbulence intensity is less than 0.1%.

The 1/4 scale heavy-class helicopter model fuselage used in the wind tunnel test activity was the same used in the GOAHEAD Project tests [7]. The GOAHEAD Project was funded by EU's Sixth Framework Programme for Research and focused on generating an advanced helicopter experimental aerodynamic database for the validation of CFD codes [8, 9]. The model internal structure was completely re-built to allow tests in both the upright and inverted configurations. In the upright configuration, the model was equipped with a rotating hub with blade stubs, thus allowing the total drag of the helicopter to be evaluated. The rotor hub represents about 40% of the complete model drag. The inverted model configuration was more appropriate for the study of the VGs positioned on the fuselage rear ramp because the VGs were not disturbed by the supporting pylon (see Fig. 1a). Similar but smaller effects on drag were found when the VGs were applied in the upright configuration that included flow disturbance from the pylon.

The wind tunnel tests were carried out in the framework of the CleanSky ROD (ROtorcraft Drag reduction) Project (part of the GRC2 Programme). This project was aimed at the evaluation of drag reduction effectiveness of the CFD-based shape optimisation performed by the GRC2 consortium on several components of the common-platform heavy-class helicopter [10]. Amongst other geometry optimizations, ONERA proposed to study four different geometries of VG arrays attached on the fuselage back-ramp [5]. The best VG configuration was determined from wind tunnel tests results obtained in cruise condition, i.e. $\alpha = -1.8°$, $\beta = 0°$. Indeed, the best configuration consisted of 8 pairs of counter-rotating VGs, as the sketch of Fig. 2 shows. Each VG had a pitch angle of $15°$, a height equal to the computed boundary layer displacement thickness δ, and a chord length equal to 3.6 δ. The VG array was built from PVC and mounted slightly downstream of the fuselage upsweep (see Fig. 1b) in the position to obtain the highest drag reduction as predicted by CFD [5] and confirmed by experiments [6]. In order to evaluate the robustness of the VG effectiveness, tests were performed with a bluff body, shaped as a radome, mounted on the fuselage lower side upstream of the VG array close to the model nose (see Fig. 1b).

A six-component RUAG 192-6L force balance installed on the head of the supporting strut was used to measure the global aerodynamic loads. The helicopter baseline fuselage drag was measured with an estimated accuracy of 0.5% of the helicopter original geometry drag in the cruise condition. The test procedure was designed to minimize the thermal drift for both the angle of attack and sideslip sweeps. Pressures were measured using more than 300 pressure taps distributed on the model fuselage. In particular, steady measurements were performed using a pressure scanner system (1 PSI F.S., accuracy 0.1% F.S.) embedded inside the model. Moreover, unsteady pressures were measured on the model back-ramp using XCS-093 Kulite miniature fast-response pressure transducers (2 PSI F.S., accuracy 0.1% F.S.). Pressures and loads were measured simultaneously for an acquisition time of 10 s for each model attitude. The acquisition frequency of unsteady pressure transducers was 10 kHz. A more detailed description of the experimental set up is given in Gibertini *et al.* [11].

Results and Discussion

The tests were performed with a wind tunnel free-stream velocity V_∞ = 50 m/s (Ma = 0.15). Sweeps of angle of attack were carried out at zero sideslip for $-14° \leq \alpha \leq 14°$ using $2°$ increments. Sideslip sweeps were performed at $\alpha = -1.8°$, corresponding to the typical cruise attitude of the tested helicopter. The loads and pressure data presented in this section are corrected for wind tunnel effects, i.e. horizontal buoyancy in the test section, supporting pylon interference and model solid blockage.

Baseline fuselage

The results of the α-sweep at $\beta = 0°$ and the β-sweep at cruise angle of attack $\alpha = -1.8°$ are shown in Figs. 3a-b for the baseline fuselage configuration. Drag coefficients (C_D) are presented as a ratio of the total helicopter drag, with rotating hub, at cruise attitude (C_{Dc}). In particular, the drag differences produced by VGs measured in the inverted configuration were added to the drag measured in the upright configuration for the complete helicopter model with rotating hub [11]. In order to highlight the effects of the VGs, Figs. 3c-d show the corresponding percentage drag difference measured for the α- and β-sweep tests.

Figures 3a and 3c show that the VGs reduce drag in the range $-4° < \alpha < 10°$. A decrease of about 2% of the complete helicopter drag (with rotating hub) was measured at cruise attitude (i.e. $\alpha = -1.8°$, $\beta = 0°$), corresponding to a reduction of more than 3% of the isolated baseline fuselage drag [6]. The maximum decrease of about 2.5% of the complete helicopter drag was measured for $\alpha = 2°$ (see Fig. 3c), close to the model attitude considered for the CFD-based optimization.

The VGs caused an increase in negative lift of about 6% for the baseline fuselage at cruise attitude. An overall reduction of the helicopter required power of the order of 0.5% was estimated taking into account both the lift and drag variations due to VGs.

The loads measured for the β-sweep tests at cruise angle of attack show that VGs are still effective for drag reduction around zero sideslip, but in a smaller range of angles with respect to the α-sweep (see Fig.

3b). In particular, as Fig. 3d clearly shows, the drag reduction due to the VGs is apparent and displays a symmetrical behavior around zero sideslip. Indeed, a sideslip variation corresponds to a modification of the VGs pitch angle (with respect to the VGs design pitch angle of $15°$), so that VGs become ineffective for a conspicuous sideslip of the model.

Based on the α- and β-sweep test results, the VGs do not introduce a drag penalty to the baseline fuselage in the range of angles outside of their operating range.

Surface pressures measured on the back-ramp surface were used to explain the flow features generated by the VGs. Figure 4a shows the position of the pressure taps on the fuselage back-ramp and the reference system used in this work (the $X - Z$ plane is located at model mid-span). The pressure taps are downstream of the VGs.

The comparison of the mean pressure coefficient (C_P) distribution measured on this fuselage section is presented in Fig. 4 for different model attitudes. When the VGs are effective for drag reduction, they produce an apparent increase of pressure on the back-ramp surface with respect to the baseline fuselage configuration, as indicated by the arrows pointing up. This pressure behavior is clearly visible from the steady measurements carried out with the model at zero angle of attack and sideslip (see Fig. 4b), as well as at cruise angle of attack and a moderate sideslip angle, i.e. $\beta = -3°$ (see Fig. 4e). This behavior is attenuated at zero sideslip and $\alpha = 8°$, where just a slight increase of the pressure distribution due to the VGs is observed (see Fig. 4c). Indeed, for these model attitudes, the VGs are suitable for limiting the suction effect responsible for pressure drag rise. Moreover, by re-energising the boundary layer, VGs prevent or limit the flow separation on the back-ramp region that increases helicopter drag.

This feature was confirmed by the unsteady pressure measurements on the back-ramp surface. Figure 5a shows the position of a sample Kulite pressure transducer on the fuselage back-ramp. Figure 5b shows the spectra comparison of the pressure signals, with and without VGs, measured at zero angle of attack and sideslip. The high degree of unsteadiness that characterizes the flow field over the back-ramp of the baseline fuselage is clearly shown with a predominant peak at $f = 21Hz$. This peak frequency corresponds to the shedding frequency of a large recirculating flow structure typical of blunt fuselages ($St = 0.28$ based on the fuselage width). On the other hand, the spectrum of the pressure signal measured with the VGs is flat, confirming the suppression of the wide separated flow region over the back-ramp.

These considerations are also supported by the results of stereo PIV surveys, described in Gibertini *et al.* [11], performed over the fuselage back-ramp region at cruise attitude with and without the VG array.

For the test conditions where the VGs are ineffective for drag reduction, the pressure distributions on the back-ramp surface measured with the VGs have almost the same behavior measured for the baseline fuselage. This observation is confirmed for large negative fuselage attitudes for example, $\alpha = -6°$, at zero sideslip (see Fig. 4d) and $\beta = -8°$, at cruise angle of attack (see Fig. 4f).

Radome effect on VGs performance

The tests carried out with the radome mounted on the model show that the VGs are ineffective in the range of angles of attack, as seen in Fig. 6a. Nevertheless, VGs do not alter the fuselage performance, as they do not produce an appreciable drag increase.

The pressure distribution measured with the radome installed confirms that no appreciable effects are introduced by VGs for the fuselage at zero angle of attack and sideslip (see Fig. 6b). Indeed, the wake of the upstream radome produces an apparent disturbance of the flow striking the VG array, nullifying their effectiveness for drag reduction. The spectra of the pressure signals measured on the fuselage back-ramp with and without the VGs have very similar behavior (see Fig. 6c), confirming that, for this case, the VGs are not effective in preserving the flow separation at the back-ramp region.

Conclusions

The use of a VG array positioned on the rear ramp of the fuselage was investigated as part of a comprehensive wind tunnel activity aimed at evaluating the effectiveness of helicopter components optimized for drag reduction. Aerodynamic loads on a heavy-class helicopter model for a range of angle of attack and sideslip angles established the limits and the robustness of the VGs to reduce fuselage drag and consequently reduce fuel consumption.

Tests results showed that an array of counter-rotating VGs positioned just downstream of the fuselage upsweep produces an appreciable drag reduction for a specific range of angles of attack and sideslip around the cruise condition, targeted by the CFD-based optimization prior to the tests. The VGs increased the pressure on the back-ramp with respect to the baseline fuselage configuration, limiting the suction effect that produces pressure drag rise. This effect was confirmed by comparing the static pressure distributions measured on the fuselage back-ramp. Moreover, unsteady pressure measurements confirmed that the VGs suppressed the wide recirculating region, characterized by a high degree of flow unsteadiness, at the junction with the tail boom.

Effectiveness of the VGs is nullified even at cruise attitude when the fuselage is equipped with a radome mounted upstream of the VGs. The wake of radome produces a flow disturbance affecting the VGs influence. Nevertheless, for the test conditions where the VGs were ineffective for drag reduction, the VGs did not introduce a drag penalty. Thus, the use of VGs can be very promising for reducing helicopters fuel consumption. In fact, they represent an inexpensive solution for obtaining a non-negligible drag reduction, while avoiding the risk of introducing a possible performance penalty for flight conditions different than cruise or for a fuselage configuration different than the baseline.

Acknowledgements

This research received funding from the European Community's Seventh Framework Programme (FP7/2007-2013) for the Clean Sky Joint Technology Initiative under grant agreement n° 325997.

References

[1]Schaeffler, N., Allan, B., Wong, O., and Tanner, P., "Experimental Investigation of Active Aerodynamic Load Reduction on a Rotorcraft Fuselage with Rotor Effects," 32nd AIAA Applied Aerodynamics Conference, Atlanta, GA, USA, June 16–20, 2014.

[2]Le Pape, A., Lienard, C., Verbeke, C., Pruvost, M., and De Coninck, J.-L., "Helicopter Fuselage Drag Reduction Using Active Flow Control: A Comprehensive Experimental Investigation," *Journal of the American Helicopter Society*, Vol. 60, (3), 2015, pp. 1–12.

[3]C., C. L., Allan, B., Le Pape, A., and Schaeffler, N., "Comparing Numerical and Experimental Results for Drag Reduction by Active Flow Control Applied to a Generic Rotorcraft Fuselage," American Helicopter Society 71th Annual Forum, Virginia Beach, VA, USA, May 5–7, 2015.

[4]Lin, J. C., “Review of research on low-profile vortex generators to control boundary-layer separation,” *Progress in Aerospace Sciences*, Vol. 38, (1), 2002, pp. 389–420.

[5]Boniface, J.-C., “A Computational Framework for Helicopter Fuselage Drag Reduction Using Vortex Generators,” AHS 70th Annual Forum, Montréal, Canada, May 20–22, 2014.

[6]Gibertini, G., Boniface, J. C., Zanotti, A., Droandi, G., Auteri, F., Gaveriaux, R., and Le Pape, A., “Helicopter drag reduction by vortex generators,” *Aerospace Science and Technology*, Vol. 47, 2015, pp. 324–339.

[7]Raffel, M., De Gregorio, F., Groot, K. D., Schneider, O., Sheng, W., Gibertini, G., and Seraudie, A., “On the generation of a helicopter aerodynamic database,” *Aeronautical Journal*, Vol. 115, (1164), 2011, pp. 103–112.

[8]Schwarz, T. and Pahlke, K., “Generation of an advanced helicopter experimental aerodynamic data base for CFD validation: The European GoAhead Project,” *Aerospace Science and Technology*, Vol. 19, (1), 2012, pp. 1–2.

[9]Antoniadis, A. F., Drikakis, D., Zhong, B., Barakos, G., Steijl, R., Biava, M., Vigevano, L., Brocklehurst, A., Boelens, O., Dietz, M., Embacher, M., and Khier, W., “Assessment of CFD methods against experimental flow measurements for helicopter flows,” *Aerospace Science and Technology*, Vol. 19, (1), 2012, pp. 86–100.

[10]Khier, W., “Computational Investigation of Advanced Hub Fairing Configurations to Reduce Helicopter Drag.” 40th European Rotorcraft Forum, Southampton, UK, September 2–5, 2014.

[11]Gibertini, G., Auteri, F., Campanardi, G., Droandi, G., Grassi, D., Le Pape, A., and Zanotti, A., “A Test Rig to Assess the Effectiveness of Drag Reduction Devices on a Heavy-Class Helicopter.” 41st European Rotorcraft Forum, Munich, Germany, September 1–4, 2015.

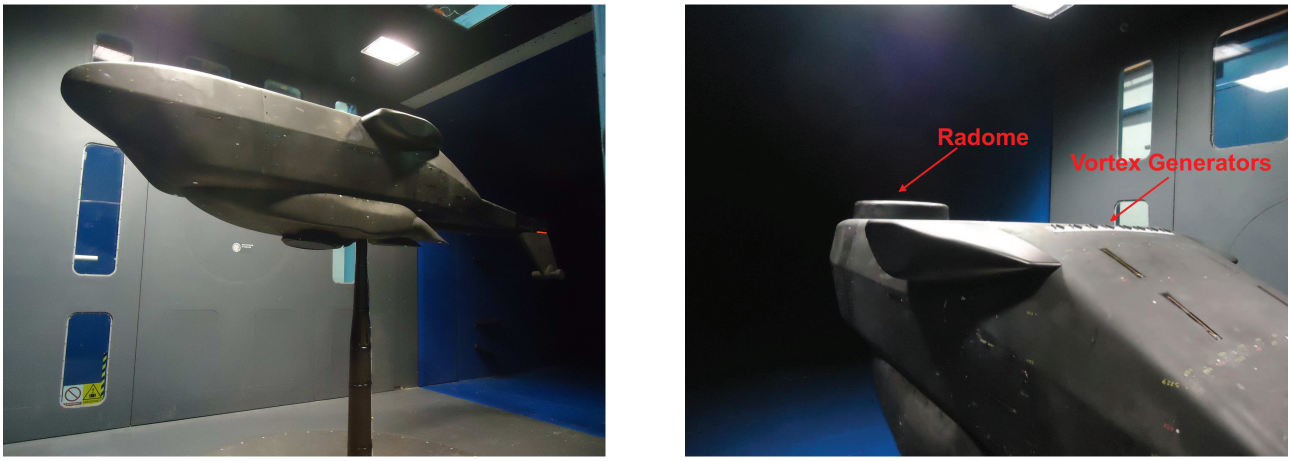

(a) (b)

Fig. 1 Helicopter fuselage model in the LGV test section: (a) inverted configuration; (b) VGs and the radome.

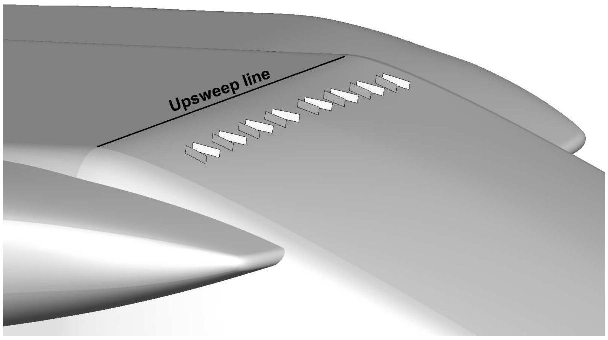

Fig. 2 Sketch of the array of 2×8 counter-rotating VGs positioned on the helicopter fuselage back-ramp.

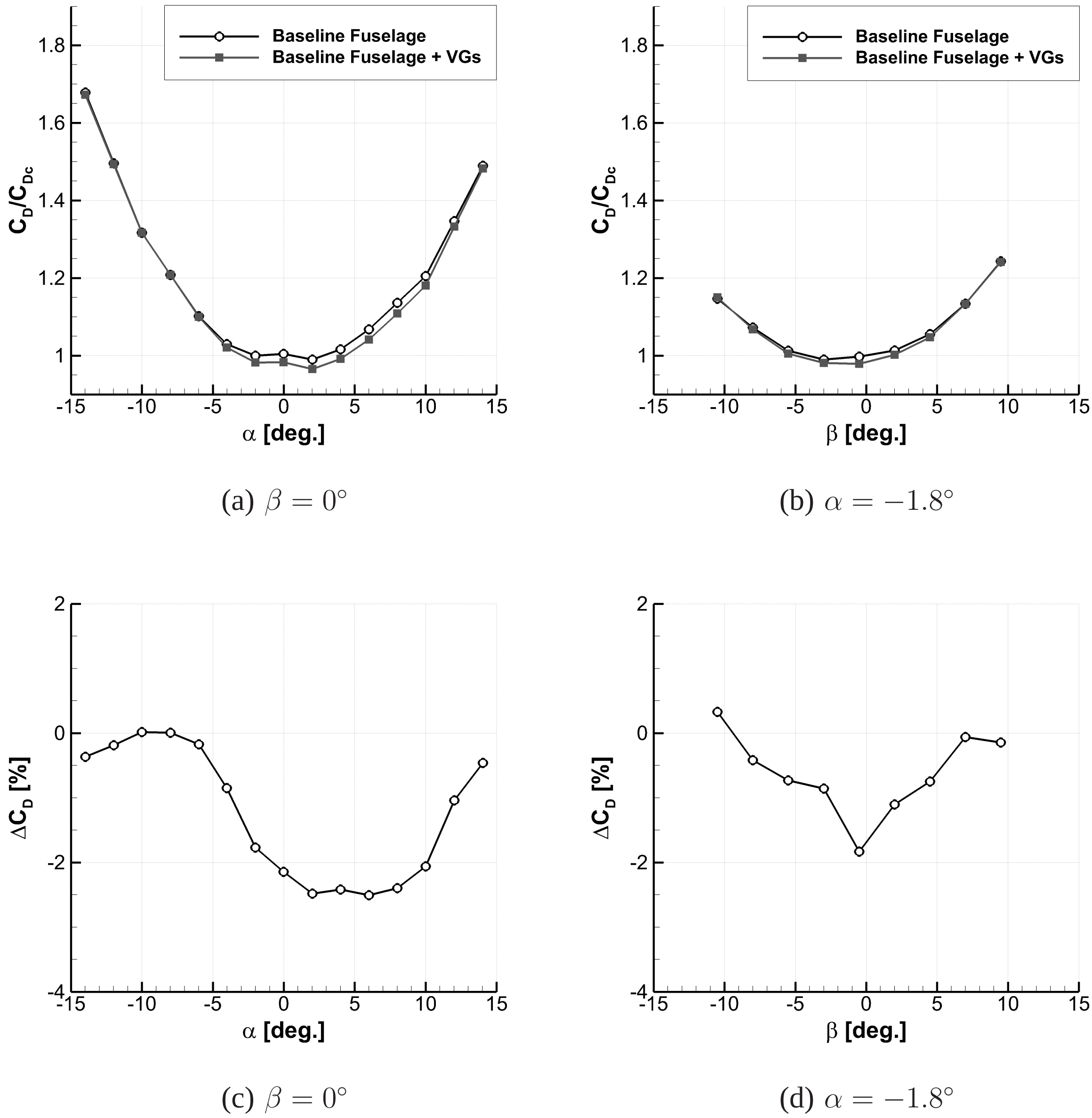

(a) $\beta = 0°$ (b) $\alpha = -1.8°$

(c) $\beta = 0°$ (d) $\alpha = -1.8°$

Fig. 3 Drag measured for $\alpha-$ and $\beta-$sweeps for M = 0.15, with and without VGs. Baseline drag was measured with model in upright position with the hub rotating. (a) drag ratio for $\alpha-$sweep at $\beta = 0°$; (b) drag ratio for $\beta-$sweep at $\alpha = -1.8°$; (c) % drag difference for $\alpha-$sweep at $\beta = 0°$; (d) % drag difference for $\beta-$sweep at $\alpha = -1.8°$.

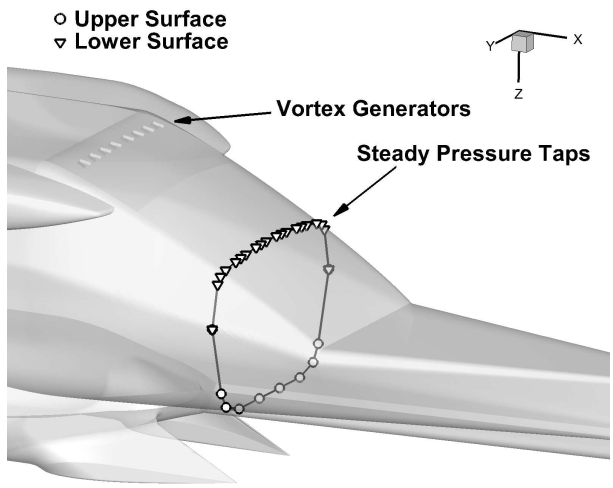

(a) Pressure taps position

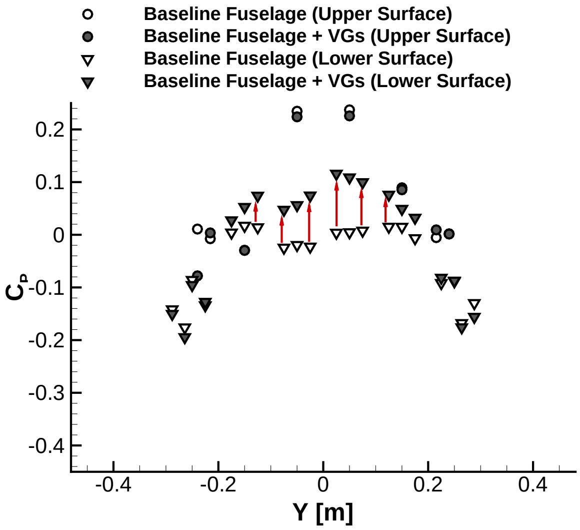

(b) $\alpha = 0°$, $\beta = 0°$

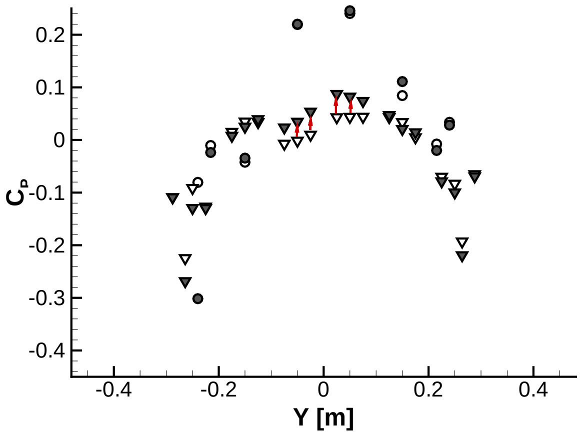

(c) $\alpha = 8°$, $\beta = 0°$

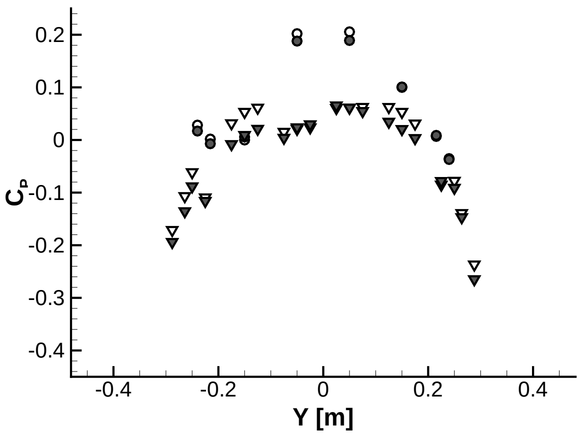

(d) $\alpha = -6°$, $\beta = 0°$

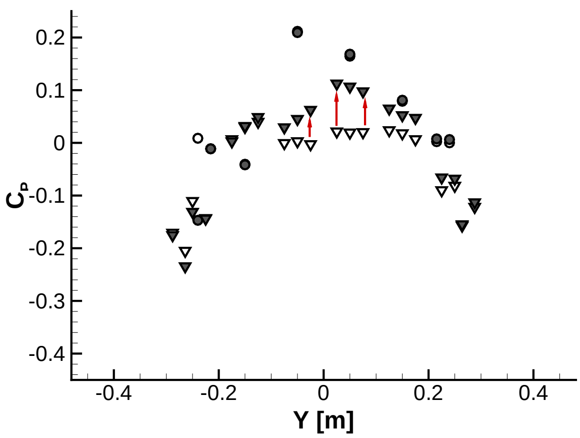

(e) $\alpha = -1.8°$, $\beta = -3°$

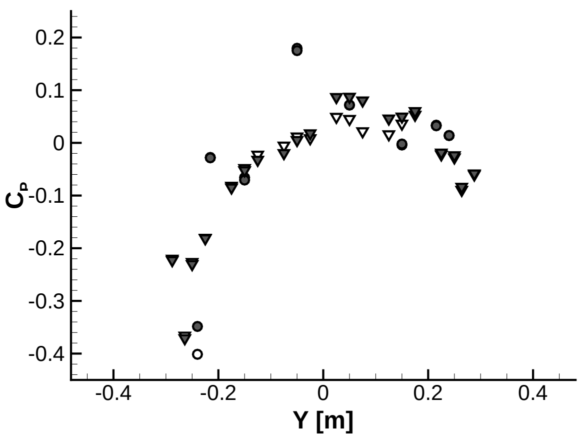

(f) $\alpha = -1.8°$, $\beta = -8°$

Fig. 4 Steady pressure measurements on fuselage back-ramp: (a) position of the pressure taps; (b-f) comparison of the pressure coefficient distribution at different fuselage attitudes.

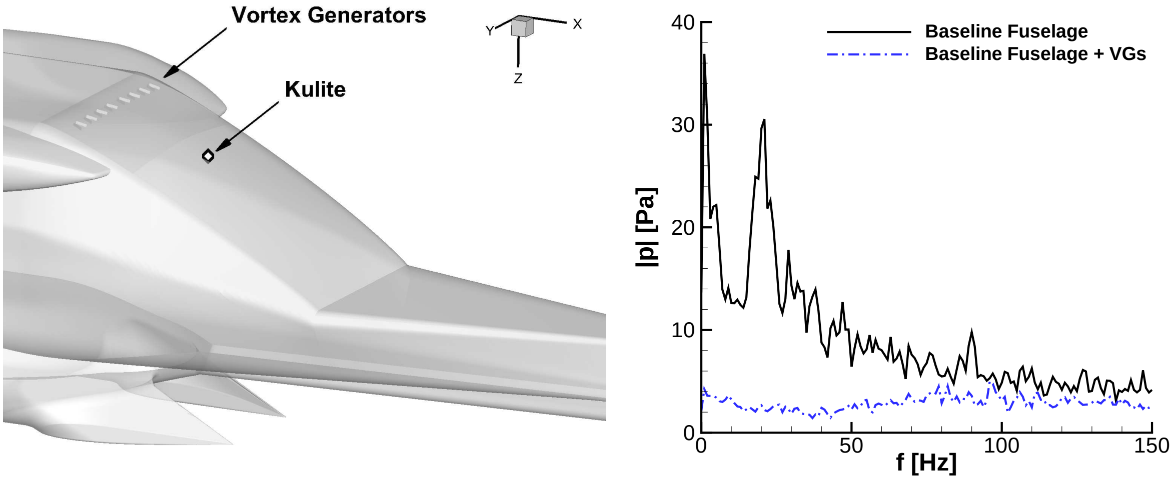

(a) Kulite position on back-ramp

(b) $\alpha = 0°$, $\beta = 0°$

Fig. 5 Unsteady pressure measurements on fuselage back-ramp: (a) position of the unsteady pressure transducer; (b) comparison of Kulite pressure signals spectra for fuselage angles of $\alpha = 0°$, $\beta = 0°$.

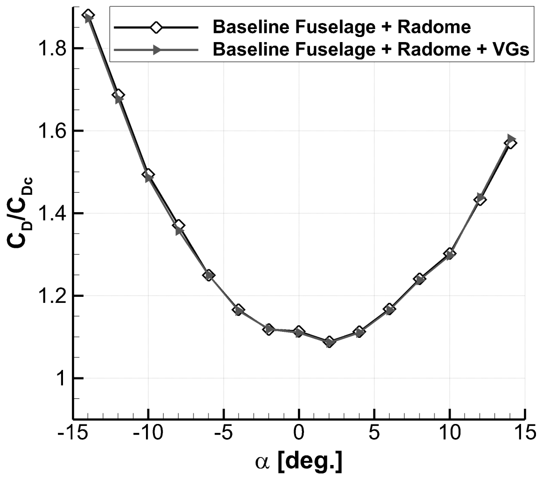

(a) $\beta = 0°$

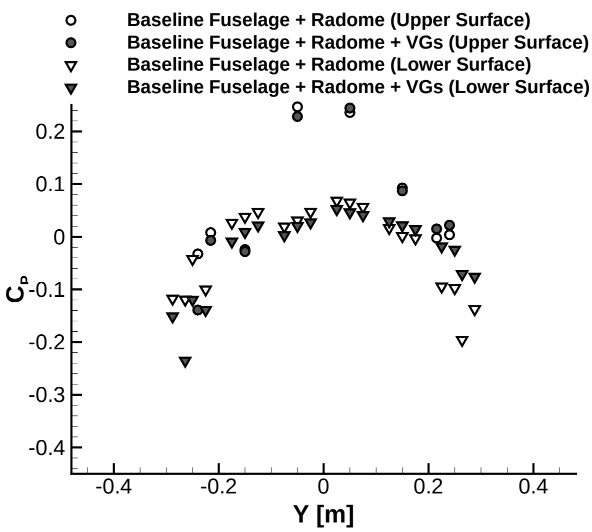

(b) $\alpha = 0°, \beta = 0°$

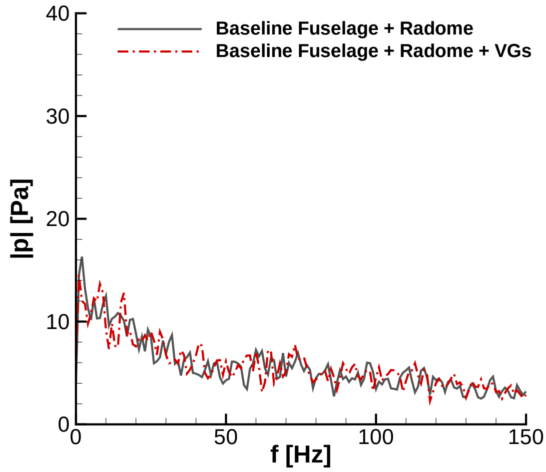

(c) $\alpha = 0°, \beta = 0°$

Fig. 6 Effect of radome on VG performance for M 0 0.15: (a) drag curves; (b) pressure coefficient distribution for $\alpha = 0°$, $\beta = 0°$; (c) unsteady Kulite pressure spectra for $\alpha = 0°$, $\beta = 0°$.